SIAM J. MATH. ANAL.
Vol. 55, No. 2, pp. 1246–1263

ASYMPTOTIC STABILITY FOR DIFFUSION WITH DYNAMIC BOUNDARY REACTION FROM GINZBURG–LANDAU ENERGY*

YUAN GAO† AND JEAN-MICHEL ROQUEJOFFRE‡

Abstract. The nonequilibrium process in dislocation dynamics and its relaxation to the metastable transition profile are crucial for understanding the plastic deformation caused by line defects in materials. In this paper, we consider the full dynamics of a scalar dislocation model in two dimensions described by the bulk diffusion equation coupled with a dynamic boundary condition on the interface, where a nonconvex misfit potential, due to the presence of dislocation, yields an interfacial reaction term on the interface. We prove that the dynamic solution to this bulk-interface coupled system will uniformly converge to the metastable transition profile, which has a bistates with fat-tail decay rate at the far fields. This global stability for the metastable pattern is the first result for a bulk-interface coupled dynamics driven only by an interfacial reaction on the slip plane.

Key words. long time behavior, metastability, algebraic decay, boundary stabilization, double well potential

MSC codes. 35K57, 35B35, 74H40

DOI. 10.1137/22M1469791

1. Introduction. Metastable pattern formations are fundamentally important processes in materials science. The associated nonequilibrium dynamics is usually determined by the internal microscopic structure but can also be approximated by a macroscopic model after incorporating some nonlinear interfacial potentials.

In this paper, we study the relaxation process to a metastable transition profile for the following full dynamics in terms of a scalar displacement function $u(t,x,y)$:

$$\begin{cases} \partial_t u - \Delta u = 0, \quad y > 0; \\ \partial_t u - \partial_y u + W'(u) = 0, \quad y = 0, \end{cases} \tag{1.1}$$

where W is a double well potential function with equal minima $W(\pm 1)$ and satisfies (1.2). Our main goal is to obtain the uniform convergence to a nontrivial steady solution, i.e., a metastable transition profile $\phi(x,y)$ connecting ± 1 at far fields $x \to \pm\infty$; see Figure 1 (right). Thus we assume that for any fixed $y \geq 0$, the initial data $u_0(x,y)$ has bistates ± 1 as $x \to \pm\infty$, which is specifically described in Assumption 1.1.

This model is motivated by nonlinear dislocation dynamics, which consists of the dynamics of the elastic continua for $y > 0$ and the nonlinear reaction induced by the interfacial misfit potential W on the slip plane $\Gamma := \{(x,y) \in \mathbb{R}^2; y = 0\}$. The static dislocation model incorporating the atomistic misfit on the interface using W was first proposed by Peierls and Nabarro [28, 34] to study the atomic core structure near the dislocation line; see Figure 1 (left) and the detailed physical derivations in

*Received by the editors January 6, 2022; accepted for publication (in revised form) September 27, 2022; published electronically April 27, 2023.
https://doi.org/10.1137/22M1469791
Funding: The first author was supported by National Science Foundation grant DMS-2204288.
†Department of Mathematics, Purdue University, West Lafayette, IN 47907 USA (gao662@purdue.edu).
‡Institut de Mathématiques de Toulouse; UMR 5219 Université de Toulouse; CNRS Université Toulouse III, 31062 Toulouse, France (jean-michel.roquejoffre@math.univ-toulouse.fr).

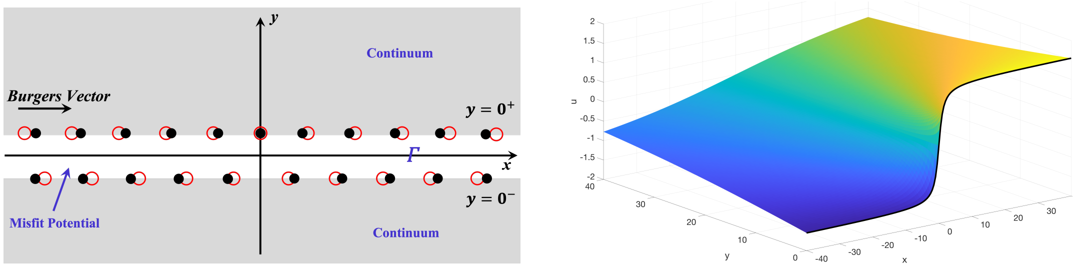

FIG. 1. *Left: Illustration of the elastic bulk continua and the atomic misfit structure at the slip plane* Γ *in the* $2D$ *Peierls–Nabarro dislocation model. The red circle is the location of atoms at the perfect reference states without deformation, while the black dots are the deformed location due to the presence of an edge dislocation at the origin. Right: The typical steady transition profile for* $\phi(x,y)$ *in* (1.4) *connecting bistates* ± 1 *on* Γ.

Appendix A. The presence of the dislocation is characterized by a nonlinear interfacial potential W on the interface Γ. Assume the double well/periodic potential W satisfies

$$\begin{aligned} &W \in C_b^3(\mathbb{R};\mathbb{R}),\\ &W(x) > W(1) = W(-1), \quad x \in (-1,1)\,,\\ &W''(\pm 1) > 0, \quad W'(\pm 1) = 0. \end{aligned} \tag{1.2}$$

For simplicity in the presentation, we also assume $W'(0) = 0$. Notice here that the unstable state 0 and the stable states ± 1 can be chosen as other generic constants without loss of generality. We remark that the double well potential only models a single transition layer connecting bistates ± 1, but a periodic potential allows possible multiple transition layers during the pattern formations [8, 20].

The motion of dislocations, the most common line defects in materials science, will lead to plastic deformations. Unlike previous related results in mathematical analysis for dislocations, which assume quasi-static elastic bulks, i.e., $\Delta u = 0$, or assume a static Lamé system for $y > 0$, the full dynamics of dislocations in (1.1) for the elastic bulks $y > 0$ and the slip plane Γ are coupled together. Physically, the fully coupled system exchanges both the mass and the energy on the bulk-boundary interface. This interaction between bulk and interface is very common in materials science, whereas the global stability analysis for the metastable equilibrium of this kind of bulk-interface interactive dynamics is absent from the literature. The global stability result in this paper will unveil the relaxation process of materials with dislocation structure. Precisely, starting from a perturbed initial data, which is probably due to impulsive stress, the full dynamics of the materials will eventually converge to a metastable steady profile. Notice there is no Dirichlet-to-Neumann map $\partial_n u = (-\Delta)^{\frac{1}{2}} u|_\Gamma$ to reduce (1.1) to a 1D nonlocal diffusion-reaction equation (see (1.13)) only on the interface Γ. Therefore in the interactive dynamics (1.1), whether all the dynamic solutions of (1.1) will uniformly converge to a single metastable transition profile (see $\phi(x,y)$) and the corresponding uniform relaxation rate are still open.

Metastable transition profile. Let us first observe a special equilibrium profile when W takes the special periodic form showing a periodic lattice property for crystal materials, i.e., $W(u) = \frac{1}{\pi^2}(1+\cos(\pi u))$. The metastable steady solution (unique up to a translation in the x direction) of

$$\begin{aligned} \Delta\phi = 0, &\quad y > 0,\\ \partial_y \phi = W'(\phi), &\quad y = 0, \end{aligned} \tag{1.3}$$

with bistates condition $\lim_{x\to\pm\infty}\phi(x,0)=\pm 1$, is given by [7, Lemma 2.1]

$$\phi(x,y)=\frac{2}{\pi}\arctan\frac{x}{y+1}; \tag{1.4}$$

see Figure 1 (right). We can easily calculate the derivatives of ϕ as

$$\partial_x\phi(x,y)=\frac{2}{\pi}\frac{y+1}{(y+1)^2+x^2},\quad \partial_y\phi(x,y)=-\frac{2}{\pi}\frac{x}{x^2+(y+1)^2}. \tag{1.5}$$

Importantly, it has been proved in [7, 30], for a general $W\in C^{2,\alpha}(\mathbb{R})$ satisfying (1.2), that there exists a unique (up to a translation in the x direction) metastable steady solution $\phi\in C^{2,\alpha}(\mathbb{R}^2_+)$ to (1.3) such that

$$\lim_{x\to\pm\infty}\phi(x,0)=\pm 1 \quad\text{ and }\quad \partial_x\phi(x,0)>0. \tag{1.6}$$

In [7, Theorem 1.6], the authors recovered the far field decay rate of the metastable profile ϕ,

$$\phi(x,0)\sim\pm 1-\frac{c}{x}\quad \text{ as } x\to\pm\infty, \tag{1.7}$$

with some constant $c>0$ and

$$|\nabla\phi(x,y)|\le\frac{c}{1+\sqrt{x^2+y^2}},\quad y\ge 0,\, x\in\mathbb{R}. \tag{1.8}$$

Here the constant c depends on only the given potential W. From now on, $c>0$ is a generic constant whose value may change from line to line but depends on only the given potential $W(x)$.

Main result and approach. Notice that the far field bistates condition $\lim_{x\to\pm\infty}\phi(x,y)=\pm 1$ for the metastable equilibrium itself is not uniformly in y. It suggests we impose the following assumptions on the initial data $u_0(x,y)$. Denote $\mathbb{R}^2_+ :=\{(x,y)\in\mathbb{R}^2; y\ge 0\}$, and denote $C_b(\mathbb{R}^2_+)$ as the space of bounded functions that are continuous up to the boundary.

Assumption 1.1. Let $\phi(x,y)$ be the unique solution (up to translation in x) to (1.3). Assume there exist constants $\xi_1,\xi_2>0$ and a function $q_0(x,y)>0$ such that

(i) q_0 satisfies

$$\lim_{x\to\pm\infty} q_0(x,y)=0 \quad\text{ uniformly in } y,\quad q_0(x,0)\in L^1(\mathbb{R})\cap L^\infty(\mathbb{R}); \tag{1.9}$$

(ii) the initial data $u_0(x,y)$ satisfies $|u_0(x,y)|<1$, and

$$\phi(x-\xi_2,y)-q_0(x,y)\le u_0(x,y)\le\phi(x+\xi_1,y)+q_0(x,y). \tag{1.10}$$

In the following theorem, we state the main result of this paper, i.e., the uniform convergence of the dynamic solution to its metastable equilibrium.

THEOREM 1.2. *Suppose the initial data $u^0(x,y)$ satisfies Assumption* 1.1. *Then the dynamic solution $u(t,x,y)$ to* (1.1) *converges to the static solution $\phi(x,y)$ of* (1.3) *in the sense that for any $\varepsilon>0$, there exist x_0 and T such that for any $t>T$,*

$$|u(t,x,y)-\phi(x-x_0,y)|<\varepsilon \quad\text{ uniformly for } (x,y)\in\mathbb{R}^2_+. \tag{1.11}$$

The key point in the proof is to construct a supersolution and a subsolution to the full dynamics (1.1) so that the full dynamics can be eventually controlled and can uniformly converge to the static profile $\phi(x, y)$ for (1.3). This generic method of constructing super-/subsolutions to study the global stability was first proposed in the pioneering work [17] for the classical 1D Allen–Cahn equation with double well potential. However, without the quasi-static assumption, one cannot reduce the full dynamics into a 1D reaction-diffusion equation (see (1.13)). Instead, the stability of the full 2D system is only ensured by an interfacial double well potential W on Γ. That is, the interface reaction activates its effect on the bulk $y > 0$ only through the Neumann boundary condition $\partial_y u$, which does not have a time-independent Dirichlet-to-Neumann map. Our construction of super-/subsolutions relies on a time decay estimate for the linearized solution $q(x, y, t)$ to (1.1) (see (3.9)), where the linearized system is also a bulk-interface interactive system. With an initial perturbation $q_0 > 0$, whose bulk part and boundary part are both nonzero, our strategy is to leverage the heat kernel in two dimensions and estimate its impact on the boundary Γ through the normal derivative $\partial_y q$. To do so, we properly decompose the linearized system as two 2D heat equations with different dynamic boundary conditions, which are coupled only through the boundary condition on Γ; see Lemma 3.2 for the algebraic decay estimate for $q(t, x, y) \lesssim \frac{1}{1+t^{\frac{3}{2}}}$.

We compare our result in Theorem 1.2 to previous results—particularly [32, 33]—on the long time behavior of dislocation dynamics with quasi-static elastic bulks. In [32, 33], the long time behavior of solutions to the reduced 1D nonlocal reaction-diffusion equation (see (1.13)) was comprehensively studied with general $(-\Delta)^{\frac{s}{2}}$ and a periodic misfit potential allowing multiple transition layers. The exponential decay from a well-prepared initial data with the same number of positively/negatively oriented dislocations to a flat constant profile was proved in [33, Theorem 1.4]. However, with a different number of oppositely oriented dislocations (called unbalanced orientation in [33]), the algebraic decay rate $1/t^{\frac{1}{2}}$ was proved in [33, Theorem 1.6], and this decay rate is due to the distance between two dislocations of $1/t^{\frac{1}{2}}$ order, and thus their polynomial fat tails produce this decay rate in the barrier function. One difference in our result is that we only focus on the long time behavior of a single transition layer, so there is no collision between dislocations. Another difference is that without the quasi-static assumption, we cannot reduce the dynamics to a 1D nonlocal equation, and we need to directly estimate the coupled dynamics in two dimensions. Thus in our result (see Theorem 1.2 and Lemma 3.2), the algebraic decay rate for the barrier function $q(t, x, y) \lesssim \frac{1}{1+t^{\frac{3}{2}}}$ comes from the interactive dynamics between the coupled elastic bulks and the transition layer on Γ. In contrast to the 1D nonlocal reaction-diffusion equation, in this paper we do not expect any exponential decay estimate for the barrier function due to the lack of the spectral gap estimate for the linearized operator L in (2.1). Indeed, due to the non-self-adjointness of L (see section 2), the spectrum of L is located in the complex plane. The spectral analysis for the coupled linear system for $q(t, x, y)$ is similar to the system (4.2), for which we are only able to find a solution with the specific upper bound of the algebraic decay rate $t^{-\frac{3}{2}}$ instead of the exponential decay. The construction of super/subsolutions for bulk-interface coupled dynamics is inspired by a series of works [5, 3, 6] on the diffusion equation with a Kolmogorov–Petrovsky–Piskunov (KPP) type reaction in the bulk and is influenced by a fast diffusion line on the boundary. However, the double well reaction $W'(u)$ in our model (1.1) presents only on the lower dimensional interface (the slip plane Γ of dislocations), which makes the uniform convergence more difficult because one wants to trap the whole half-plane dynamics using only reactions on the boundary.

State of the art. In the study of mechanical behaviors of materials with the presence of dislocations, the characterization of the equilibrium profile and the dynamic process, as well as the corresponding relaxation rate for the dynamics to the equilibrium state, has proceeded in various directions at the level of mathematical analysis. In [7], Cabré and Solà-Morales S-M established the existence and uniqueness (up to translations) of monotonic solutions and also proved that the metastable profile is a local minimizer of the corresponding free energy,

$$E(u) := \frac{1}{2}\int_{\mathbb{R}^2_+} |\nabla u|^2 \,\mathrm{d}x\,\mathrm{d}y + \int_\Gamma W(u)\,\mathrm{d}x. \tag{1.12}$$

Later, Palatucci, Savin, and Valdinoci [30] directly proved the existence of the reduced nonlocal equation $(-\Delta)^{\frac{1}{2}}u|_\Gamma = -W'(u)$ on Γ, which is derived via the Dirichlet- to-Neumann map $\partial_n u = (-\Delta)^{\frac{1}{2}}u|_\Gamma$. Very recently, in [12] the authors proved the rigidity for a class of 3D vectorial dislocation models, which states that the equilibrium profile has to be a 1D profile with uniform displacement in the $z$direction. Moreover, using an elastic extension, in [23] the authors rigorously connect the 2D Lamé system with the nonlinear boundary condition to the 1D reduced nonlocal equation. For the dynamics of dislocations, existing results only work under a quasi-static assumption for the elastic bulks in $y > 0$ so that one can still use the Dirichlet-to-Neumann map to reduce the quasi-static dynamics to a 1D nonlocal reaction-diffusion equation,

$$\partial_t u + (-\Delta)^{\frac{1}{2}}u = -W'(u) \quad \text{on } \Gamma. \tag{1.13}$$

In [20], the long time behavior of the single edge dislocation and its exponential relaxation was proved via a new notion of an ω-limit set. At the macroscopic scale, the 1D slow motion of N-dislocations was studied in [24]; see also general cases including collisions of dislocation transition profiles with opposite orientations in [31, 32, 33] and for general fractional Laplacian $(-\Delta)^{\frac{s}{2}}\tilde{u}$ with $0 < s < 2$ in [10, 11]. These 1D results for the quasi-static model are motivated by the pioneering works [2, 8, 9, 17] for the classical 1D local Allen–Cahn equation. For bulk-interface dynamics, such as the Fisher-KPP diffusion-reaction coupled with an interfacial diffusion, [3, 4, 5, 6, 35] studied the propagation of fronts, which is closely related to our bulk-interface dynamics but with a KPP type reaction appearing in the bulk instead of on the interface.

In the remainder of this paper, we first briefly explain in section 2 why a solution to (1.1) exists; then the asymptotic behavior is described in the remaining three sections. We prove the key estimates for the construction of supersolutions/subsolutions in section 3. These rely on a decomposition for the dynamic boundary condition and a heat kernel computation, which is developed in section 4. Then in section 5, we complete the proof of the main convergence result, Theorem 1.2. The gradient flow derivations for the bulk-interface dynamics (1.1) is shown in Appendix A.

2. C_0-semigroup and existence of dynamic solutions. As a preliminary, in this section we first clarify that the linear operator for (1.1) is not self-adjoint and that the theory of C_0-semigroup solution for semilinear equations ensures the existence of a dynamic solution to (1.1).

Without the nonlinear term W, regarding (1.1) as a Kolmogorov forward equation, Feller explicitly characterized the generator L with domain $D(L)$ of a contraction semigroup in [15, 16]; see also [36]. These pioneering works in the 1950s first identified all admissible boundary conditions for a second order differential operator L to generate a contraction semigroup on a properly chosen Banach space. Denote $C(\overline{\mathbb{R}^2_+})$ as the space of continuous functions u in $\{(x,y)\in\mathbb{R}^2; y\geq 0\}$ such that there exists a finite limit for u at far fields. For any test function $f\in C^2_b(\overline{\mathbb{R}^2_+})$, $L: D(L)\subset C(\overline{\mathbb{R}^2_+})\to C(\overline{\mathbb{R}^2_+})$ is defined as

$$Lf := \begin{cases} \Delta f, & x\in\mathbb{R}^2_+, \\ -\partial_n f, & x\in\Gamma, \end{cases} \tag{2.1}$$

with the domain

$$D(L) = \{f\in C^2_b(\overline{\mathbb{R}^2_+}); \Delta f = -\partial_n f \text{ for } x\in\Gamma\}.$$

Then the full dynamics (1.1) in a matrix form will be

$$\partial_t \begin{pmatrix} u \\ u_\Gamma \end{pmatrix} = Lu + \begin{pmatrix} 0 \\ -W'(u) \end{pmatrix} =: \mathcal{L}u, \quad u(x,0)=u_0(x). \tag{2.2}$$

Although L is symmetric, it is not self-adjoint, and the spectral analysis is more delicate. Indeed, the adjoint operator $L^*: D(L^*)\subset L^1(\mathbb{R}^2_+)\times L^1(\Gamma)\to L^1(\mathbb{R}^2_+)\times L^1(\Gamma)$ is given by

$$L^*\rho := \begin{cases} \Delta\rho, & x\in\mathbb{R}^2_+, \\ -\partial_n\rho, & x\in\Gamma. \end{cases} \tag{2.3}$$

The domain of the adjoint L^* has been characterized in [15] as

$$D(L^*) = \{(\rho,\rho_\Gamma)\in L^1(\mathbb{R}^2_+)\times L^1(\Gamma); \rho\in W^{2,1}(\mathbb{R}^2_+)\}. \tag{2.4}$$

Here we notice that for dimension $n=2$, the trace theorem implies $W^{2,1}(\mathbb{R}^2_+)\hookrightarrow L^q(\Gamma)$ for any $1\leq q<+\infty$. Thus the trace ρ_Γ is well defined.

There are many results on the fact that the linear operator L generates a strongly continuous semigroup on the product space $L^1(\mathbb{R}^2_+)\otimes L^1(\Gamma)$ or on $C(\overline{\mathbb{R}^2_+})\otimes C(\Gamma)$. For instance, the associated Feller semigroup on $C(\overline{\mathbb{R}^2_+})$ was studied in [15, 16]; see also [1, 13] for bounded domain $\overline{\Omega}$, and see detailed investigations in [25, Proposition 9, Theorem 7] for half-space $\overline{\mathbb{R}^2_+}$. Since $W(\cdot)\in C^3_b(\mathbb{R})$, the semigroup solution for the quasi-linear (2.2) can be obtained by proving that for some $\omega>0$ large enough, $\mathcal{L}-\omega I$ is the generator of a strongly continuous semigroup of contraction. Although the existence of dynamic solutions is not the focus of this paper, we refer the reader to [14, 18, 19, 27, 37, 38] for existence results of various kinds on dynamic boundary condition problems.

3. Construction of supersolutions and subsolutions. In this section, we will give the crucial supersolution/subsolution estimates for the dynamic solution in Proposition 3.1. This relies on a detailed decay estimate for the corresponding linearized bulk-interface dynamics; see Lemma 3.2. Compared with the classical local/nonlocal diffusion-reaction equation, the decay rate with respect to time t becomes an algebraic rate due to the bulk-interface interaction.

Recall the full dynamics (1.1),

$$\begin{cases} \partial_t u - \Delta u = 0, & y>0; \\ \partial_t u - \partial_y u + W'(u) = 0, & y=0. \end{cases}$$

Let $\phi(x,y)$ be the metastable equilibrium solution to (1.3). Then we know ϕ satisfies (1.6)–(1.8). The goal of this section is to use ϕ to construct a supersolution and a subsolution to (1.1) so that the dynamic solution is approximately squeezed between two static transition profiles provided time is large enough.

Recall the double well potential W satisfies (1.2). This interfacial misfit potential $W(\cdot)$ on slip plane Γ has two local minimums ± 1, which essentially determines and drives the whole dislocation dynamics to the metastable transition profile $\phi(x,y)$. Let us first clarify some properties of W. Since $W''(\pm 1) > 0$, there exist constants $\mu > 0$, $\delta > 0$ such that

$$\begin{aligned} &W'(\phi+q) - W'(\phi) \geq \mu q \quad \text{for } 1-\delta \leq \phi \leq 1,\ 0<q<\delta, \\ &W'(\phi+q) - W'(\phi) \geq \mu q \quad \text{for } -1 \leq \phi \leq -1+\delta,\ 0<q<1-\delta. \end{aligned} \tag{3.1}$$

Here in the second line of (3.1), we used the facts that $W'(-1)=0$, $W'(x)>0$ for $-1<x<0$ and $\phi+\delta<0$. Moreover, for $\phi \in [-1+\delta, 1-\delta]$, there exist constants $k>0$, $\beta \geq 0$ such that

$$|W'(\phi-q) - W'(\phi)| \leq kq, \tag{3.2}$$

and by (1.6),

$$\partial_x \phi(x,0) \geq \beta > 0 \quad \text{for } x \text{ such that } \phi(x) \in [-1+\delta, 1-\delta]. \tag{3.3}$$

Next, in Proposition 3.1 we state the crucial comparison principle for the dynamic solution to (1.1). The proof of this proposition relies on the properties of the interfacial potential, and the proof of Lemma 3.2 relies on the decay estimate of the linearized bulk-interface dynamics. Lemma 3.2 ensures that one can trap the full dynamics using merely an interfacial double well potential. We will first give the proof of Proposition 3.1 in this section, and then give the proof of Lemma 3.2 in the next section.

Proposition 3.1 (construction of supersolutions/subsolutions). *Let $u(t,x,y)$ be the solution to bulk-interface dynamics* (1.1) *with initial data $u_0(x,y)$. Suppose the initial data $u_0(x,y)$ satisfies Assumption* 1.1. *Then there exist constants ξ_1, ξ_2, $C>0, M>0$, and $q_0(x,y)>0$ such that*

$$\phi(x-\xi_2+2M(1+t)^{-\frac{1}{2}},y) - \frac{q_0(x,y)}{1+Ct^{\frac{3}{2}}} \leq u(t,x,y) \leq \phi(x+\xi_1-2M(1+t)^{-\frac{1}{2}},y) + \frac{q_0(x,y)}{1+Ct^{\frac{3}{2}}}, \tag{3.4}$$

where $\phi(x,y)$ is the steady profile satisfying (1.3).

Proof. We will construct a supersolution as

$$\bar{u}(t,x,y) := \min\{1, \phi(x+\xi(t),y) + q(t,x,y)\} \in [-1,1] \tag{3.5}$$

by choosing $\xi(t)$ and $q(t,x,y) \geq 0$. The construction of the subsolution is similar.

Step 1. For u_0 satisfying Assumption 1.1, there exists a number $\tilde{\xi}_1 > 0$ such that

$$u_0(x,y) \leq \phi(x+\tilde{\xi}_1, y) + q_0(x,y), \tag{3.6}$$

and $0<q_0<1$, $\lim_{x\to\pm\infty} q_0(x,y) = 0$ uniformly in y.

We need to choose $\xi(t)$ and $q(t,x,y)$ such that

$$\begin{aligned} \partial_t \bar{u} - \Delta \bar{u} \geq 0, &\quad y>0; \\ \partial_t \bar{u} - \partial_y \bar{u} + W'(\bar{u}) \geq 0, &\quad y=0. \end{aligned} \tag{3.7}$$

Here the equations hold in the viscosity sense. Since the minimum of two viscosity supersolutions (indeed, classical supersolutions for our case) is still a viscosity supersolution, we don't need to verify the viscosity supersolution test for nondifferentiable points brought by the minimum in (3.5). Thus , we only verify the equations in the classical sense on differentiable points. We refer the reader to [5] for details on the comparison principle of this type of generalized supersolution.

From the steady solution to (1.3), we know that $\Delta\phi = 0$ for $y > 0$ and $\partial_y \phi = W'(\phi)$ on $y = 0$. Therefore we obtain

(3.8)
$$\begin{aligned}
&\partial_t \bar{u} - \Delta \bar{u} = \partial_x \phi(x+\xi(t), y)\xi' + \partial_t q - \Delta q \qquad \text{for } y > 0;\\
&\partial_t \bar{u} - \partial_y \bar{u} + W'(\bar{u})\\
&\quad = \partial_x \phi(x+\xi(t), 0)\xi' + \partial_t q - \partial_y q - W'\big(\phi(x+\xi(t),0)\big) + W'\big(\phi(x+\xi(t),0)+q\big)\\
&\qquad\quad \text{for } y = 0.
\end{aligned}$$

Here, the function $\xi(t)$ with $\xi' \geq 0$ will be chosen explicitly in Step 3.

Now we choose $q(t,x,y)$ with $0 < q_0(x,y) < 1$ such that

$$\begin{aligned}
\partial_t q - \Delta q = 0, \quad y > 0,\\
\partial_t q - \partial_y q + \mu q = 0, \quad y = 0,
\end{aligned} \tag{3.9}$$

where $\mu > 0$ is the constant in (3.1).

Step 2. To prove $\bar{u}$ is a supersolution, divide the space into several sets,

$$\begin{aligned}
I_1 &:= \{(t,x,y); \phi(x+\xi(t),y) \in [1-q, 1]\},\\
I_2 &:= \{(t,x,y); \phi(x+\xi(t),y) \in [1-\delta, 1-q]\},\\
I_3 &:= \{(t,x,y); \phi(x+\xi(t),y) \in [-1+\delta, 1-\delta]\},\\
I_4 &:= \{(t,x,y); \phi(x+\xi(t),y) \in [-1, -1+\delta]\}.
\end{aligned}$$

Here, some sets being empty is allowed. We now estimate the right-hand side of (3.8) for both the bulk and the interface in all possible cases as follows.

Case (i): If $(t,x,y) \in I_1$, then $\phi(x+\xi(t),y) + q(t,x,t) \geq 1$ and $\bar{u} \equiv 1$.

Case (ii): If $(t,x,y) \in I_2$ or $(t,x,y) \in I_4$, then from (3.1),

$$-W'(\phi(x+\xi(t),0)) + W'(\phi(x+\xi(t),0)+q) \geq \mu q \qquad \text{for some } \mu > 0. \tag{3.10}$$

Thus using (3.9), we have on $y = 0$,

$$\partial_t \bar{u} - \partial_y \bar{u} + W'(\bar{u}) \geq \partial_x \phi(x+\xi(t),y)\xi' + \partial_t q - \partial_y q + \mu q = \partial_x \phi(x+\xi(t),y)\xi' =: R_1, \tag{3.11}$$

and for $y > 0$,

$$\partial_t \bar{u} - \Delta \bar{u} = \partial_x \phi(x+\xi(t),y)\xi' + \partial_t q - \Delta q = R_1. \tag{3.12}$$

Here, we used the equations for q in (3.9). Since the profile ϕ is increasing with respect to x, we know $R_1 \geq 0$ and conclude that (3.7) holds.

Case (iii): If $(t,x,y) \in I_3$, then from (3.2) we have on $y = 0$,

$$\partial_t \bar{u} - \partial_y \bar{u} + W'(\bar{u}) \geq \beta \xi' + \partial_t q - \partial_y q - kq =: R_2. \tag{3.13}$$

Since q satisfies (3.9), $R_2 \geq 0$ if and only if

$$\xi' \geq \frac{-\partial_t q + \partial_y q + kq}{\beta} = \frac{(\mu+k)q}{\beta}. \tag{3.14}$$

Therefore, to prove $\bar{u}$ is a supersolution, we only need the following lemma to estimate the decay of $q(t,x,0)$. The proof of Lemma 3.2 will be given later in section 4.

LEMMA 3.2. *Let q be the solution to (3.9) with initial data $0<q_0<1$; then there exists $C>0$ such that*

$$|q(t,x,y)| \le \frac{q_0(x,y)}{1+Ct^{\frac{3}{2}}}. \tag{3.15}$$

Step 3 As a consequence of Lemma 3.2 and (3.14), we can choose

$$\xi(t) = \tilde{\xi}_1 + 2M - 2M(1+t)^{-\frac{1}{2}} = \xi_1 - 2M(1+t)^{-\frac{1}{2}}$$

satisfying $\xi'(t) = M(1+t)^{-\frac{3}{2}}$ with $M>0$ large enough such that (3.14) holds. Thus we obtain that $\bar{u}$ is a supersolution and conclude that (3.4) holds. The construction of the subsolution is similar; we omit the details.

From the proof of Proposition 3.1, we see that the construction relies on a time decay estimate (3.15) for the linearized bulk-interface coupled dynamics (3.9).

4. The proof of Lemma 3.2. In this section, we give the proof of the key decay estimates in Lemma 3.2 for the linearized system (3.9). The proof consists of (i) decomposing the bulk-interface coupled linear system as two heat equations with different dynamic boundary conditions, and (ii) estimating the boundary stabilization rate for each subproblem.

Step 1. Since the initial data q_0 has both nonzero bulk part and interface part, we first choose a proper decomposition of q to decouple the dynamics for $y>0$ and $y=0$.

Assume the initial data $q_0(x,y)$ can be expressed as a bulk part and an interface part,

$$q_0(x,y) = q_0\chi_{y>0} + q_0\chi_{y=0} =: q_0^b(x,y) + q_0^s(x), \tag{4.1}$$

where χ is the characteristic function. We perform the Laplace transform of $q(t,x,y)$ with respect to t using Laplace variable λ and carry out the Fourier transform with respect to x using Fourier variable η and denote it as $\hat{q} := \hat{q}(\lambda,\eta,y)$. Then $\hat{q}$ satisfies

$$\begin{aligned} \lambda\hat{q} - \partial_{yy}\hat{q} + \eta^2\hat{q} &= \hat{q}_0^b, \quad y>0,\\ \lambda\hat{q} - \partial_y\hat{q} + \mu\hat{q} &= \hat{q}_0^s, \quad y=0, \end{aligned} \tag{4.2}$$

where $\hat{q}_0^b = \hat{q}_0^b(\eta,y)$ (resp., $\hat{q}_0^s = \hat{q}_0^s(\eta)$) is the Fourier transform of $q_0^b(x,y)$ (resp., $q_0^s(x)$) with respect to x. Since the equations for q are linear, we can construct $q = q_1 + q_2$ with $\hat{q} = \hat{q}_1 + \hat{q}_2$ such that $\hat{q}_1$ satisfies

$$\begin{aligned} &\lambda\hat{q}_1 - \partial_{yy}\hat{q}_1 + \eta^2\hat{q}_1 = 0, && y>0,\\ &\lambda\hat{q}_1 - \partial_y\hat{q}_1 + \mu\hat{q}_1 = \hat{q}_0^s + \partial_y\hat{q}_2, && y=0, \end{aligned} \tag{4.3}$$

while $\hat{q}_2$ satisfies

$$\begin{aligned} \lambda\hat{q}_2 - \partial_{yy}\hat{q}_2 + \eta^2\hat{q}_2 &= \hat{q}_0^b, \quad y>0,\\ \hat{q}_2(\lambda,\eta,0) &= 0, \quad y=0. \end{aligned} \tag{4.4}$$

One can first solve $\hat{q}_2$ and then $\hat{q}_1$ with the dynamic boundary input from q_2.

Step 2. Estimate q_1 and q_2 separately.

First, for a solution $\hat{q}_2$ satisfying (4.4), one can directly estimate the solution q_2 to the heat equation for $y>0$ with initial data q_0^b and Dirichlet boundary condition $q_2(t,x,0)=0$ on $y=0$. Denote $\bar{q}_0^b$ as the odd extension of q_0^b to the whole space $\mathbb{R}^2$, and denote $\Phi(t,x,y)=\frac{1}{4\pi t}e^{-\frac{x^2+y^2}{4t}}$ as the 2D fundamental solution to the heat equation in $\mathbb{R}^2$. Then the solution formula for q_2 is given by $q_2=\Phi * \bar{q}_0^b$. Since $|\partial_y\Phi|\le \frac{cy}{t^2}e^{-\frac{x^2+y^2}{4t}}$, by using the change of variable $s=\frac{y^2}{4t}$, we obtain

$$|\partial_y q_2| \le c\int_0^{+\infty}\int_{\mathbb{R}} |\partial_y \Phi|\,\mathrm{d}x\,\mathrm{d}y \le c\int_{\mathbb{R}} \frac{1}{t^{\frac12}} e^{-\frac{x^2}{4t}}\,\mathrm{d}x \int_0^{+\infty} \frac{1}{t^{\frac12}} e^{-s}\,\mathrm{d}s \le \frac{c}{t^{\frac12}}. \tag{4.5}$$

Second, we estimate solution $\hat{q}_1$ satisfying (4.3). Since we seek solutions with far field decay as $y\to+\infty$, the solution $\hat{q}_1$ to (4.3) can be represented by

$$\hat{q}_1(\lambda,\eta,y)=\hat{q}_1(\lambda,\eta,0)e^{-\sqrt{\lambda+\eta^2}\,y}. \tag{4.6}$$

From (4.3) and (4.4), we know q_1 satisfies the boundary condition

$$\partial_y \hat{q}_1(\lambda,\eta,0) = -\sqrt{\eta^2+\lambda}\,\hat{q}_1(\lambda,\eta,0) = (\lambda+\mu)\hat{q}_1(\lambda,\eta,0) - \hat{q}^s_{2in}(\lambda,\eta), \tag{4.7}$$

where

$$\hat{q}^s_{2in}(\lambda,\eta) := \hat{q}^s_0(\eta) + \partial_y \hat{q}_2(\lambda,\eta,0), \qquad q^s_{2in}(t,x) := q^s_0(x) + \partial_y q_2(t,x,0). \tag{4.8}$$

Therefore,

$$\hat{q}_1(\lambda,\eta,0)=\frac{\hat{q}^s_{2in}(\lambda,\eta)}{\lambda+\mu+\sqrt{\lambda+\eta^2}}. \tag{4.9}$$

Then by inverse transform we obtain

$$q_1(t,x,0)=c q^s_{2in}(t,x) * \int_\Upsilon \int_{\mathbb{R}} e^{\lambda t}\frac{e^{ix\eta}}{\lambda+\mu+\sqrt{\lambda+\eta^2}}\,\mathrm{d}\eta\,\mathrm{d}\lambda, \tag{4.10}$$

where Υ is the vertical line from $Re(\lambda)-Ti$ to $Re(\lambda)+Ti$ with $T\to+\infty$, and $Re(\lambda)$ is greater than any singularities of $\int_{\mathbb{R}} \frac{e^{ix\eta}}{\lambda+\mu+\sqrt{\lambda+\eta^2}}\,\mathrm{d}\eta$.

Third, fixing $t>0$, we now estimate the $L^\infty(\mathbb{R})$ norm for $q_1(t,x,0)$.

Observe that the branch point $\lambda=-\eta^2$ is a singularity. Then take the branch cut $(-\infty,-\eta^2)$ and set $\lambda=-\eta^2+re^{i\theta}$ with $-\pi\le\theta<\pi$, $r>0$. We calculate the roots of $\lambda+\mu+\sqrt{\lambda+\eta^2}=0$ for $r>0$. It is sufficient to solve

$$\begin{aligned} \mu-\eta^2+r\cos\theta+\sqrt{r}\cos\frac{\theta}{2}&=0,\\ r\sin\theta+\sqrt{r}\sin\frac{\theta}{2}&=0. \end{aligned} \tag{4.11}$$

For $-\pi\le\theta<\pi$, (4.11) indeed has no solution if $\eta^2<\mu$, while if $\eta^2\ge\mu$, (4.11) has only one solution,

$$\theta=0, \quad r+\sqrt{r}=\eta^2-\mu. \tag{4.12}$$

This shows that we can take Υ as any vertical line such that

$$0 > Re(\lambda) > r^* - \eta^2 = -\sqrt{r^*} - \mu, \tag{4.13}$$

where r^* is the solution to (4.12).

To estimate the complex integral $\int_\Upsilon \int_{\mathbb{R}} e^{\lambda t} \frac{e^{ix\eta}}{\lambda+\mu+\sqrt{\lambda+\eta^2}} \,\mathrm{d}\eta\,\mathrm{d}\lambda$, we only need to consider two cases, i.e., (i) $\eta^2 \geq \mu$ and (ii) $\eta^2 < \mu$. For (ii), since there is no singularity in the complex integral, by Cauchy's integral theorem and standard calculations, it is sufficient to estimate the complex integral for one piece of the contour, i.e.,

$$C_1 := \left\{ \lambda = -\eta^2 + \varepsilon e^{i\theta}, \quad -\frac{\pi}{2} < \theta < \frac{\pi}{2} \right\}.$$

For (i), to avoid the singularity at $\lambda = -\eta^2 + r^*$, it is sufficient to estimate the complex integral for one piece of the contour, i.e.,

$$C_2 := \left\{ \lambda = -\mu + \varepsilon e^{i\theta}, \quad -\frac{\pi}{2} < \theta < \frac{\pi}{2} \right\}.$$

Next, we explain detailed estimates for these two cases.

Case (i). For $\eta^2 \geq \mu$, from (4.13) we can always choose $Re(\lambda) \ll -\varepsilon$, which gives the exponential decay with respect to t,

$$\begin{aligned} &\left\| \int_{C_2} \int_{\mathbb{R}} e^{\lambda t} \frac{e^{ix\eta}}{\lambda + \mu + \sqrt{\lambda+\eta^2}} \,\mathrm{d}\eta\,\mathrm{d}\lambda \right\|_{L^1_x(\mathbb{R})} \\ &\leq c e^{-\mu t} \left\| \int_{\mathbb{R}} e^{-(\sqrt{\alpha t}\eta - \frac{ix}{2\sqrt{\alpha t}})^2} e^{\alpha \eta t} e^{-\frac{x^2}{4\alpha t}} \,\mathrm{d}\eta \right\|_{L^1_x(\mathbb{R})} \leq c e^{-\frac{\mu}{2} t} \end{aligned} \tag{4.14}$$

for $\alpha > 0$ small enough and $t > 0$ large enough. Thus for any $t > 0$ large enough, from (4.10) and Young's convolution inequality, we obtain the uniform estimate for q_1,

$$\begin{aligned} \|q_1(t,x,0)\|_{L^\infty_x} &\leq \|q^s_{2in}(t,x)\|_{L^\infty_x} \left\| \int_\Upsilon \int_{\mathbb{R}} e^{\lambda t} \frac{e^{ix\eta}}{\lambda+\mu+\sqrt{\lambda+\eta^2}} \,\mathrm{d}\eta\,\mathrm{d}\lambda \right\|_{L^1_x} \\ &\leq \left\| q^s_0(x) + \frac{1}{\sqrt{t}} \right\|_{L^\infty_x} \left\| \int_\Upsilon \int_{\mathbb{R}} e^{\lambda t} \frac{e^{ix\eta}}{\lambda+\mu+\sqrt{\lambda+\eta^2}} \,\mathrm{d}\eta\,\mathrm{d}\lambda \right\|_{L^1_x} \leq c e^{-ct}. \end{aligned} \tag{4.15}$$

Here, in the second inequality we used the definition of q^s_{2in} in (4.8) and the estimate (4.5), while in the last inequality we used (4.14).

Case (ii). For $\eta^2 < \mu$, we shall be careful about the region where $\eta^2 \ll 1$ and $0 > Re(\lambda) > -\varepsilon$; otherwise, we still have the exponential decay as in (4.15). Denote $\xi = \sqrt{t}\eta$ and $z = \varepsilon e^{i\theta}$; then

$$\begin{aligned} |q_1(t,x,0)| &\leq \left| c q^s_{2in}(t,x) * \frac{1}{\mu} \int_{C_1} \int_{|\eta|\leq 1} e^{-\lambda t + ix\eta} \,\mathrm{d}\eta\,\mathrm{d}\lambda \right| \\ &= \left| c q^s_{2in}(t,x) * \frac{1}{\mu} \int_{-\frac{\pi}{2}}^{\frac{\pi}{2}} \int_{|\eta|\leq 1} e^{-\eta^2 t + \varepsilon e^{i\theta} t + ix\eta} \,\mathrm{d}\eta\,\mathrm{d}\theta \right| \\ &\leq \left| \frac{c}{\mu} \frac{1}{t^{\frac{3}{2}}} q^s_{2in}(t,x) * \int_{\mathbb{R}} e^{-\xi^2 + i\frac{x\xi}{\sqrt{t}}} \,\mathrm{d}\xi \right| \\ &\leq \left| \frac{c}{t^{\frac{3}{2}}} (q^s_{2in}(t,x) * e^{-\frac{x^2}{2t}}) \int_{\mathbb{R}} e^{-\frac{(\xi - \frac{xi}{\sqrt{2t}})^2}{2}} \,\mathrm{d}\xi \right|, \end{aligned} \tag{4.16}$$

where the factor $\frac{1}{t^{\frac{3}{2}}}$ comes from the change of variables $\xi=\sqrt{t}\eta$ and $\tilde{z}=zt$. Then from the definition of q_{2in}^s in (4.8), the estimate (4.5), and Young's convolution inequality, we obtain

$$\begin{aligned}\|q_1(t,x,0)\|_{L_x^\infty} \le& \frac{c}{t^{\frac{3}{2}}}\left\|[q_0^s(x)+\partial_y q_2(t,x,0)] * e^{-\frac{x^2}{2t}}\right\|_{L_x^\infty}\\ \le&\frac{c}{t^{\frac{3}{2}}}\left\|q_0^s(x) * e^{-\frac{x^2}{2t}}+\frac{1}{\sqrt{t}} * e^{-\frac{x^2}{2t}}\right\|_{L_x^\infty}\\ \le&\frac{c}{t^{\frac{3}{2}}}\left(\|q_0^s\|_{L_x^1}+\frac{1}{\sqrt{t}}\|e^{-\frac{x^2}{2t}}\|_{L_x^1}\right)\le\frac{c}{t^{\frac{3}{2}}}.\end{aligned}\tag{4.17}$$

In this last inequality, we used $\|e^{-\frac{x^2}{2t}}\|_{L_x^1}\le ct^{\frac{1}{2}}$.

Step 3. Combine estimates for q_1 and q_2 to estimate $q(t,x,0)$ and $q(t,x,y)$.

First from (4.7) and $\hat{q}_2(\lambda,\eta,0)=0$, we have on $y=0$

$$\partial_y\hat{q}=\partial_y\hat{q}_1+\partial_y\hat{q}_2=-\sqrt{\eta^2+\lambda}\,\hat{q}_1+\partial_y\hat{q}_2=-\sqrt{\eta^2+\lambda}\,\hat{q}+\partial_y\hat{q}_2.\tag{4.18}$$

This, together with the boundary condition for $\hat{q}$ in (4.2), yields that on $y=0$,

$$\left(\lambda+\mu+\sqrt{\eta^2+\lambda}\right)\hat{q}-\partial_y\hat{q}_2=\hat{q}_0^s.\tag{4.19}$$

Therefore from (4.8) and all cases discussed in Step 2, one have for t large enough,

$$\|q(t,x,0)\|_{L_x^\infty}=\left\|cq_{2in}^s * \int_\Upsilon\int_{\mathbb{R}} e^{\lambda t}\frac{e^{ix\eta}}{\lambda+\mu+\sqrt{\lambda+\eta^2}}\,\mathrm{d}\eta\,\mathrm{d}\lambda\right\|_{L_x^\infty}\le\frac{c}{t^{\frac{3}{2}}},\tag{4.20}$$

where Υ is the same path as (4.10). Thus from the maximal principle for the heat equation, we conclude that the solution q to (3.9) satisfies the estimate (3.15).

Remark 1. Suppose the assumption for the initial data changes to the following: Assume the initial data $u_0(x,y)=\phi(x-x_0,y)+q_0(x,y)$ for some x_0 and $q_0(x,0)$ satisfies $\|q_0(x,0)\|_{L_x^p(\mathbb{R})}\le c$ for some $1<p<\infty$. Then (4.17) becomes $\|q_1(t,x,0)\|_{L_x^\infty(\mathbb{R})}\le\frac{c}{t^{1+\frac{1}{2p}}}$. Indeed, from the interpolation inequality, we know that

$$\|e^{-\frac{x^2}{2t}}\|_{L_x^q}\le\|e^{-\frac{x^2}{2t}}\|_{L_x^1}^{\frac{1}{q}}\|e^{-\frac{x^2}{2t}}\|_{L_x^\infty}^{1-\frac{1}{q}}\le ct^{\frac{1}{2q}}\tag{4.21}$$

for $1<q<\infty$. Then by Young's convolution inequality, we obtain

$$\left\|q_0^s(x) * e^{-\frac{x^2}{2t}}\right\|_{L_x^\infty}\le\left\|q_0^s\right\|_{L_x^p}\|e^{-\frac{x^2}{2t}}\|_{L_x^q}\le ct^{\frac{1}{2q}}\tag{4.22}$$

for $\frac{1}{p}+\frac{1}{q}=1$. Therefore,

$$\|q_1(t,x,0)\|_{L_x^\infty}\le\frac{c}{t^{\frac{3}{2}}}\left\|q_0^s * e^{-\frac{x^2}{2t}}+\frac{1}{\sqrt{t}} * e^{-\frac{x^2}{2t}}\right\|_{L_x^\infty}\le\frac{c}{t^{1+\frac{1}{2p}}}.\tag{4.23}$$

As a consequence, in (3.14) we can choose $\xi(t)=\xi_1-2pMt^{-\frac{1}{2p}}$ with $\xi'(t)=Mt^{-1-\frac{1}{2p}}$ and $M>0$ large enough such that (3.14) holds.

5. Proof of Theorem 1.2: Uniform convergence to metastable equilibrium. The crucial comparison principle obtained in Proposition 3.1 helps us to control the dynamic solution between two steady transition profiles as time becomes large enough. In this section, combining Proposition 3.1 with the energy dissipation law (A.5), we prove the uniform convergence of the dynamic solution of (1.1) to the equilibrium $\phi(x,y)$.

Proof of Theorem 1.2. *Step* 1. From the boundedness of initial data u^0 and smoothness of the nonlinear potential W, by the parabolic interior regularity, the solution u to (1.1) satisfies the following uniform bounds:

$$|u| \le c, \quad |\nabla u| \le c, \quad |D^2 u| \le c. \tag{5.1}$$

Then from the Arzela–Ascoli theorem, for any bounded set B_k there exist $u^*(x,y)$ and $t^k_{n_k}$ such that as $n_k \to +\infty$,

$$u(t^k_{n_k},\cdot,\cdot) \to u^*(\cdot,\cdot) \quad \text{uniformly in } B_k. \tag{5.2}$$

Then by a diagonal argument, there exists a subsequence t^ℓ_ℓ such that as $\ell \to +\infty$,

$$u(t^\ell_\ell,\cdot,\cdot) \to u^*(\cdot,\cdot) \quad \text{uniformly in } B_\ell. \tag{5.3}$$

Step 2. From Proposition 3.1, we know for $(x,y) \in B^c_\ell$, it also holds that

$$\phi(x-\xi_2+2M(1+t)^{-\frac{1}{2}},y)-\frac{q_0(x,y)}{1+Ct^{\frac{3}{2}}} \le u(x,y) \le \phi(x+\xi_1-2M(1+t)^{-\frac{1}{2}},y)+\frac{q_0(x,y)}{1+Ct^{\frac{3}{2}}}. \tag{5.4}$$

Combining (5.4) with the uniform decay of $|\nabla \phi|$ in (1.8), we know there exists N large enough such that for any $\ell > N$ and for any fixed c,

$$|u(t^\ell_\ell,x,y)-\phi(x-c,y)| < \varepsilon \quad \text{uniformly in } B^c_\ell. \tag{5.5}$$

This, together with (5.3), shows that for any $\varepsilon > 0$, there exists N large enough such that for any $\ell > N$,

$$|u(t^\ell_\ell,x,y)-u^*(x,y)| < \varepsilon \quad \text{uniformly for } (x,y) \in \mathbb{R}^2_+, \tag{5.6}$$

and there exist constants c_1, c_2 such that u^* satisfies

$$\phi(x-c_2,y)-\varepsilon \le u^*(x,y) \le \phi(x-c_1,y)+\varepsilon. \tag{5.7}$$

Step 3. Recall the total energy E defined in (1.12) for system (1.1). Note the energy dissipation law (A.5) for dynamic solution u,

$$\dot{E}(t) = -Q(t) \le 0.$$

Now we claim there is a lower bound for $E(t)$ provided t is large enough. Indeed, the first term in E is positive, while the second term in E is bounded,

$$
\begin{aligned}
&\left|\int_\Gamma W(u)\,\mathrm{d}x\right| \\
&= \Big| \int_{y=0,x>0} W'(1)(u-1)\,\mathrm{d}x + \int_{y=0,x>0} W''(\xi)(u-1)^2\,\mathrm{d}x \\
&+ \int_{y=0,x<0} W'(-1)(u+1)\,\mathrm{d}x + \int_{y=0,x<0} W''(\xi)(u+1)^2\,\mathrm{d}x \Big| \\
&\le c\int_{y=0,x>0} (u-1)^2\,\mathrm{d}x + c\int_{y=0,x<0}(u+1)^2\,\mathrm{d}x,
\end{aligned}
\tag{5.8}
$$

where we used properties for W in (1.2). Then combining the decay rate of $\phi(x,0)$ in (1.7) with (5.4), for $u(t^\ell_\ell)$ with t^ℓ_ℓ large enough, we know that

$$
\left|\int_\Gamma W(u)\,\mathrm{d}x\right| \le c\int_\Gamma \frac{1}{(1+x)^2}\,\mathrm{d}x \le c. \tag{5.9}
$$

This implies a lower bound for $E(t)$ provided t is large enough. Therefore there exists a subsequence (still denoted as t^ℓ_ℓ) such that when $t^\ell_\ell \to +\infty$, we must have $Q(t^\ell_\ell)\to 0$. Thus we know that

$$
\begin{aligned}
\liminf_{t^\ell_\ell\to 0} \int_{\mathbb{R}^2_+} |\Delta u|^2\,\mathrm{d}x\,\mathrm{d}y \le \liminf_{t^\ell_\ell\to 0} Q(t^\ell_\ell) = 0,\\
\liminf_{t^\ell_\ell\to 0} \int_\Gamma |\partial_y u - W'(u)|^2\,\mathrm{d}x \le \liminf_{t^\ell_\ell\to 0} Q(t^\ell_\ell) = 0.
\end{aligned}
\tag{5.10}
$$

This, together with (5.6) and Fatou's lemma, yields that the limit u^* satisfies the static equation (1.3). From the uniqueness (up to a translation in x) of static problem (1.3), we know $u^*(x,y)=\phi(x-x_0,y)$ for some x_0.

Step 4. Combining with the small data stability due to Proposition 3.1, we know for any $\varepsilon>0$ there exists T such that for any $t>T$,

$$
|u(t,x,y)-\phi(x-x_0,y)|<\varepsilon \quad \text{uniformly for } (x,y)\in\mathbb{R}^2_+. \tag{5.11}
$$

This concludes the uniform convergence result in Theorem 1.2. ∎

We further remark that the uniform convergence result is a global stability result for a single metastable transition profile $\phi(x,y)$. For a slow bulk diffusion coupled with fast boundary reaction system, one can also use this global stability result for a single profile to study the pattern formation of an N multilayer transition profile at a finite time. This will rely on obtaining a localized version for the uniform stability result in Theorem 1.2, which also is based on the fat tail estimate for the transition profile ϕ. We will leave the multilayer pattern formation and its slow motion persistence as a future study.

Appendix A. Vectorial dislocation model with an interfacial misfit energy. We briefly introduce the physical model and the associated total energy for dislocations. Then we derive the 2D bulk-interface interactions through gradient flows of a simplified total energy E in (1.12). The associated energy dissipation law (A.5) is important for the proof of the uniform convergence of the dynamic solution.

A dislocation core is a microscopic region of heavily distorted atomistic structures with shear displacement jump across a slip plane $\Gamma := \{(x,y,z); y=0\}$. The propagation of a dislocation core, i.e., distorted displacement profile, will eventually lead to plastic deformation with a low energy barrier. The classical dislocation theory regards the dislocation core as a singular point and uses linear elasticity theory to compute the dislocation profile; see [26, Chapters 2 and 3] for detailed modeling in both isotropic and anistropic media and the linear deformation response due to dislocations. Instead, the Peierls–Nabarro model introduced by Peierls and Nabarro [28, 34] is a multiscale continuum model for displacement $\mathbf{u} = (u_1, u_2, u_3)$ that incorporates the atomistic effect by introducing a nonlinear interfacial potential W on the slip plane Γ. Two elastic continua $y > 0$ and $y < 0$ are connected by the nonlinear atomistic potential $W([u_1])$ depending on shear displacement jump $[u_1]$ across the slip plane Γ; see Figure 1 (left). To minimize the elastic energy and the misfit energy induced by dislocation, the steady solution to the Peierls–Nabarro model is the minimization problem

$$\begin{aligned}\text{(A.1)}\qquad \mathbf{u} &= \operatorname{argmin}\{E_{\text{elastic}}(\mathbf{u}) + E_{\text{misfit}}(\mathbf{u})\}\\ &= \operatorname{argmin}\left\{\frac{1}{2}\int_{\mathbb{R}^3\setminus\Gamma} \sigma : \varepsilon \,\mathrm{d}x\,\mathrm{d}y\,\mathrm{d}z + \int_\Gamma W([u_1])\,\mathrm{d}x\,\mathrm{d}z\right\},\end{aligned}$$

among all displacements fields $\mathbf{u}$ with bistates far field condition $[u_1](\pm\infty) = \pm 2$, where ε is the strain tensor, σ is the stress tensor, and $\varepsilon : \sigma := \sum_{i,j} \varepsilon_{ij}\sigma_{ij}$. Here W is a Ginzburg–Landau type potential on the interface which determines the stable states for the shear displacement and drives metastable pattern formation; see (1.2). Without loss of generality, we assume a symmetric displacement in the upper/lower elastic bulks and fix the total magnitude of the dislocation, so the minimization constraint in (A.1) can be simplified to that for any z, $\lim_{x\to\pm\infty} u_1(x, 0, z) = \pm 1$. The following simplified total energy (see (1.12)) in terms of the scalar shear displacement function $u = u_1(x, y, z)$ is commonly used in mathematical analysis:

$$\text{(A.2)}\qquad E(u) = \frac{1}{2}\int_{\mathbb{R}^2_+} |\nabla u|^2 \,\mathrm{d}x\,\mathrm{d}y + \int_\Gamma W(u)\,\mathrm{d}x.$$

For a straight dislocation with uniform displacement in the z direction, the equivalence between the minimizers of the simplified energy E and of the original physical energy in (A.1) is proved in [23]. Meanwhile, if the misfit potential depends on only the shear jump displacement across the slip plane Γ, then the rigidity result in [12, 22] shows that the steady solution must be a straight dislocation with a 1D profile. Therefore, we will use the simplified total energy (1.12) to derive and study the full dynamics of dislocations expressed in terms of scalar displacement $u(x, y)$. However, the full dynamics and global stability for the true vectorial dislocation model make up a challenging future project.

Model derivation via gradient flow. In this section, we derive the bulk-interface interactive dynamics (1.1) via gradient flow of the total energy (1.12). Recall the upper half-plane

$$\text{(A.3)}\qquad \mathbb{R}^2_+ := \{(x, y) \in \mathbb{R}^2; y > 0\}; \quad \overline{\mathbb{R}^2_+} := \{(x, y) \in \mathbb{R}^2; y \geq 0\}.$$

Denote $\Gamma := \{(x, y); y = 0\}$, $u|_\Gamma = u(x, 0)$.

The full dynamics of dislocation motion is essentially determined by the total energy and how the energy changes against frictions for the bulks and on the slip plane. First, one can compute the rate of change of total energy with respect to any virtual velocity $\dot{u}$. Then one determines the true velocity by Onsager's linear response theory with proper energy dissipation relation [29]; see, in particular, Onsager's linear response theory for obstacle problems in [21]. Here, we use the simplest quadratic Rayleigh dissipation functional to include frictions in the bulks and on slip plane Γ as the dissipation metric in $\overline{\mathbb{R}^2_+}$.

For any velocities $\dot{u}, \dot{v}$, choose the quadratic Rayleigh dissipation functional,

$$g(\dot{u},\dot{v}) := \int_{\mathbb{R}^2_+} \dot{u}\dot{v}\,\mathrm{d}x\,\mathrm{d}y + \int_\Gamma \dot{u}_\Gamma \dot{v}_\Gamma\,\mathrm{d}x.$$

Here, without loss of generality, we take same friction coefficients for the bulk velocity and for its trace on slip plane Γ. Then the gradient flow of E with respect to metric $g(\cdot,\cdot)$ is $g(\partial_t u, \dot{u}) = -\frac{\mathrm{d}}{\mathrm{d}\varepsilon}\big|_{\varepsilon=0} E(u+\varepsilon\dot{u})$ for any virtual velocity $\dot{u}$. After calculating the first variation of E, this gradient flow reads

$$\begin{aligned} g(\partial_t u, \dot{u}) &= -\frac{\mathrm{d}}{\mathrm{d}\varepsilon}\Big|_{\varepsilon=0} E(u+\varepsilon\dot{u}) \\ &= \int_{\mathbb{R}^2_+} \nabla u \nabla \dot{u}\,\mathrm{d}x\,\mathrm{d}y + \int_\Gamma W'(u)\dot{u}\,\mathrm{d}x \\ &= -\int_{\mathbb{R}^2_+} \Delta u \dot{u}\,\mathrm{d}x\,\mathrm{d}y + \int_\Gamma [\partial_n u + W'(u)]\dot{u}\,\mathrm{d}x. \end{aligned} \tag{A.4}$$

Then by taking arbitrary virtual velocity $\dot{u}$, we conclude with the governing equation (1.1). From the same calculations as in (A.4), we also have the energy dissipation law,

$$\begin{aligned} \frac{\mathrm{d}}{\mathrm{d}t}E(u) &= \int_{\mathbb{R}^2_+} \nabla u \nabla u_t\,\mathrm{d}x\,\mathrm{d}y + \int_\Gamma W'(u) u_t\,\mathrm{d}x \\ &= -\int_{\mathbb{R}^2_+} u_t^2\,\mathrm{d}x\,\mathrm{d}y - \int_\Gamma u_t^2\,\mathrm{d}x \\ &= -\int_{\mathbb{R}^2_+} |\Delta u|^2\,\mathrm{d}x\,\mathrm{d}y - \int_\Gamma [\partial_y u - W'(u)]^2\,\mathrm{d}x =: -Q(t) \le 0. \end{aligned} \tag{A.5}$$

REFERENCES

[1] W. Arendt, G. Metafune, D. Pallara, and S. Romanelli, *The Laplacian with Wentzell-Robin boundary conditions on spaces of continuous functions*, Semigroup Forum, 67 (2003), pp. 247–261, https://doi.org/10.1007/s00233-002-0010-8.

[2] P. W. Bates, P. C. Fife, X. Ren, and X. Wang, *Traveling waves in a convolution model for phase transitions*, Arch. Ration. Mech. Anal., 138 (1997), pp. 105–136.

[3] H. Berestycki, A.-C. Coulon, J.-M. Roquejoffre, and L. Rossi, *The effect of a line with nonlocal diffusion on Fisher-KPP propagation*, Math. Models Methods Appl. Sci., 25 (2015), pp. 2519–2562, https://doi.org/10.1142/S0218202515400175.

[4] H. Berestycki, R. Ducasse, and L. Rossi, *Influence of a road on a population in an ecological niche facing climate change*, J. Math. Biol., 81 (2020), pp. 1059–1097.

[5] H. Berestycki, J.-M. Roquejoffre, and L. Rossi, *The influence of a line with fast diffusion on Fisher-KPP propagation*, J. Math. Biol., 66 (2013), pp. 743–766, https://doi.org/10.1007/s00285-012-0604-z.

[6] H. Berestycki, J.-M. Roquejoffre, and L. Rossi, *The shape of expansion induced by a line with fast diffusion in Fisher-KPP equations*, Commun. Math. Phys., 343 (2016), pp. 207–232, https://doi.org/10.1007/s00220-015-2517-3.

[7] X. Cabré and J. Solà-Morales, *Layer solutions in a half-space for boundary reactions*, Commun. Pure Appl. Math., 58 (2005), pp. 1678–1732, https://doi.org/10.1002/cpa.20093.

[8] J. Carr and R. L. Pego, *Metastable patterns in solutions of $u_t = \epsilon^2 u_{xx} - f(u)$*, Commun. Pure Appl. Math., 42 (1989), pp. 523–576.

[9] X. Chen, *Generation, propagation, and annihilation of metastable patterns*, J. Differ. Equ., 206 (2004), pp. 399–437, https://doi.org/10.1016/j.jde.2004.05.017.

[10] S. Dipierro, A. Figalli, and E. Valdinoci, *Strongly nonlocal dislocation dynamics in crystals*, Comm. Partial Differential Equations, 39 (2014), pp. 2351–2387.

[11] S. Dipierro, G. Palatucci, and E. Valdinoci, *Dislocation dynamics in crystals: A macroscopic theory in a fractional Laplace setting*, Comm. Math. Phys., 333 (2015), pp. 1061–1105.

[12] H. Dong and Y. Gao, *Existence and uniqueness of bounded stable solutions to the peierls-nabarro model for curved dislocations*, Calc. Var. Partial Differerential Equations, 60 (2021), pp. 1–26.

[13] K.-J. Engel, *The Laplacian on $C(\overline{\varpi})$ with generalized Wentzell boundary conditions*, Arch. Math., 81 (2003), pp. 548–558, https://doi.org/10.1007/s00013-003-0557-y.

[14] A. Favini, G. R. Goldstein, J. A. Goldstein, and S. Romanelli, *C_0 -semigroups generated by second order differential operators with general Wentzell boundary conditions*, Proc. Amer. Math. Soc., 128 (2000), pp. 1981–1989, https://doi.org/10.1090/S0002-9939-00-05486-1.

[15] W. Feller, *The parabolic differential equations and the associated semi-groups of transformations*, Ann. of Math. (2) 55, (1952), pp. 468–519.

[16] W. Feller, *Diffusion processes in one dimension*, Trans. Amer. Math. Soc., 77 (1954), pp. 1–31.

[17] P. C. Fife and J. B. McLeod, *The approach of solutions of nonlinear diffusion equations to traveling wave solutions*, Arch. Ration. Mech. Anal., 65 (1977), pp. 355–361.

[18] Y. Gao, J. Liang, and T.-J. Xiao, *Observability inequality and decay rate for wave equations with nonlinear boundary conditions*, Electron. J. Differential Equations, 2017 (2017), pp. 1–12.

[19] Y. Gao, J. Liang, and T.-J. Xiao, *A new method to obtain uniform decay rates for multidimensional wave equations with nonlinear acoustic boundary conditions*, SIAM J. Control Optim., 56 (2018), pp. 1303–1320, https://doi.org/10.1137/16M107863X.

[20] Y. Gao and J.-G. Liu, *Long time behavior of dynamic solution to Peierls-Nabarro dislocation model*, Methods Appl. Anal., 27 (2020), pp. 161–198, https://doi.org/10.4310/MAA.2020.v27.n2.a4.

[21] Y. Gao and J.-G. Liu, *Projection method for droplet dynamics on groove-textured surface with merging and splitting*, SIAM J. Sci. Comput., 44 (2022), pp. B310–B338, https://doi.org/10.1137/20M1338563.

[22] Y. Gao, J.-G. Liu, and Z. Liu, *Existence and rigidity of the Peierls–Nabarro model for dislocations in high dimensions*, Nonlinearity, 34 (2021), pp. 7778–7828, https://doi.org/10.1088/1361-6544/ac24e3.

[23] Y. Gao, J.-G. Liu, T. Luo, and Y. Xiang, *Revisit of the Peierls-Nabarro model for edge dislocations in Hilbert space*, Discrete Contin. Dyn. Syst. B, 26 (2021), pp. 3177–3207.

[24] M. González and R. Monneau, *Slow motion of particle systems as a limit of a reaction-diffusion equation with half-Laplacian in dimension one*, Discrete Contin. Dyn. Syst., 32 (2012), pp. 1255–1286.

[25] D. Guidetti, *Linear parabolic problems with dynamic boundary conditions in spaces of Hölder continuous functions*, Ann. Math. Pure Appl., 195 (2016), pp. 167–198, https://doi.org/10.1007/s10231-014-0457-8.

[26] J. P. Hirth and J. Lothe, *Theory of Dislocations* , 2nd ed., Wiley, New York, 1982.

[27] M. Mokhtar-Kharroubi and Q. Richard, *Time asymptotics of structured populations with diffusion and dynamic boundary conditions*, Discrete Contin. Dyn. Syst. B, 23 (2018), pp. 4087–4116, https://doi.org/10.3934/dcdsb.2018127.

[28] F. Nabarro, *Dislocations in a simple cubic lattice*, Proc. Phys. Soc., 59 (1947), pp. 256–272.

[29] L. Onsager, *Reciprocal relations in irreversible processes* I, Phys. Rev., 37 (1931), pp. 405–426, https://doi.org/10.1103/PhysRev.37.405.

[30] G. Palatucci, O. Savin, and E. Valdinoci, *Local and global minimizers for a variational energy involving a fractional norm*, Ann. Math. Pura Appl., 192 (2013), pp. 673–718, https://doi.org/10.1007/s10231-011-0243-9.

[31] S. Patrizi and E. Valdinoci, *Crystal dislocations with different orientations and collisions*, Arch. Ration. Mech. Anal., 217 (2015), pp. 231–261.

[32] S. Patrizi and E. Valdinoci, *Relaxation times for atom dislocations in crystals*, Calc. Var. Partial Differential Equations, 55 (2016), pp. 1–44.

[33] S. Patrizi and E. Valdinoci, *Long-time behavior for crystal dislocation dynamics*, Math. Models Methods Appl. Sci., 27 (2017), pp. 2185–2228.

[34] R. Peierls, *The size of a dislocation*, Proc. Phys. Soc., 52 (1940), pp. 34–37.

[35] L. Rossi, A. Tellini, and E. Valdinoci, *The effect on Fisher-KPP propagation in a cylinder with fast diffusion on the boundary*, SIAM J. Math. Anal., 49 (2017), pp. 4595–4624, https://doi.org/10.1137/17M1125388.

[36] A. D. Venttsel', *On boundary conditions for multidimensional diffusion processes*, Theory Probab. Appl., 4 (1959), pp. 164–177, https://doi.org/10.1137/1104014.

[37] J. L. Vázquez and E. Vitillaro, *Heat equation with dynamical boundary conditions of reactive type*, Commun. Partial Differential Equations, 33 (2008), pp. 561–612, https://doi.org/10.1080/03605300801970960.

[38] T.-J. Xiao and J. Liang, *Second order differential operators with Feller-Wentzell type boundary conditions*, J. Funct. Anal., 254 (2008), pp. 1467–1486, https://doi.org/10.1016/j.jfa.2007.12.012.